Materials Research. 2019; 22(suppl. 1): e20180786
DOI: http://dx.doi.org/10.1590/1980-5373-MR-2018-0786

Study of the Plastic Deformation of API 5L X80 Steel Exposed to the Microbiological Action of Produced Water

***Edkarlla Sousa Dantas de Oliveira*[a]*, *Roseana Florentino da Costa Pereira*[a], *Maxime Montoya*[a], *Maria Alice Gomes de Andrade Lima*[b], *Severino Leopoldino Urtiga Filho*[a]**

[a]*Universidade Federal de Pernambuco, Departamento de Engenharia Mecânica, Avenida Professor Moraes Rego, 1235, Cidade Universitária, Recife, PE, Brasil*
[b]*Universidade Federal de Pernambuco, Departamento de Engenharia Química, Av. Prof. Arthur Sá, s/n, Cidade Universitária, Recife, PE, Brasil*

Received: December 4, 2018; Revised: August 20, 2019; Accepted: December 5, 2019

The mechanical behavior of the API 5L X80 steel exposed to the produced water by the petroleum industry, besides being dependent on the intrinsic properties of the steel, is influenced by the corrosivity characteristics of the electrolyte that may be associated with the presence of microorganisms. The objective of this work was to investigate the plastic deformation of API 5L X80 steel exposed to produced water. The tests were conducted in static systems (abiotic and biotic) containing produced water after 360 days. The process of corrosion of the coupons were evaluated by topographic 3D analysis and roughness, and the mechanical behavior by tensile test and fracture analysis by scanning electron microscopy. Surface topography and roughness were modified by the interaction of the consortium of microorganisms with the substrate associated with the corrosion process. The results indicate that microorganisms induced the formation of pits which caused the coupons to lose plasticity.

Keywords: *API 5L X80 steel, mechanical behavior, microorganisms, produced water.*

1. Introduction

Currently, the use of high-strength and low-alloy carbon steels (HSLA) has been growing in the petroleum industry due to their high resistance to stresses, good toughness and good weldability owing to a combination of low carbon and thermo-mechanical manufacturing processes. A classification of steels indicated for the transport of oil and gas is specified in API 5L standard, the steel in this study is classified as API 5L X80, which in addition to the properties inherent in its class, presents high resistance to corrosion when exposed to the oil industry fluids[1,2]. Studies on low alloy steel report that the depending on the level of the alloying elements (silicon and sulfur) in the chemical composition of the material coupled with the presence of microorganisms in the aqueous medium to which it is exposed increases the susceptibility to corrosion[3]. The exposure of metallic structures such as pipelines to the fluids of the petroleum industry, mainly produced water, has been the subject of numerous studies due to its predisposition to corrosive phenomena. The nature of the corrosive environment can be modified by the action of microorganisms[4]. Several microorganisms such as bacteria, fungi and algae can be found in the produced water. Futhermore, it presents high salinity, droplets of dispersed oils, minerals, organic compounds and radioactive materials responsible for the harmful effects of corrosion during the oil secondary recovery process[5,6]. The literature reports studies correlating the combined action of stresses and microbiological activity causing changes in the corrosion behavior of X80 steel. Wu et al. studied the synergistic effects of the elastic stress associated with the action of sulfate reducing bacteria (SRB) on API 5L X80 steel. The experiments showed that SRB favored the initial formation of pits in the steel increasing the corrosion. It was observed that the elastic tension maintained and promoted the growth of this pitting[7]. Wu et al. evaluated SRB activity on X80 steel under yield stress. The results showed the formation of secondary pits on the bottom of wide shallow pits through the SRB microbiological activity. When SRB were associated with yield stress, it was observed that steel corrosion was increased by the growth of micro-cracks and localized corrosion[8]. There are studies evaluating the mechanical alterations of the X80 steel after the exposure to sulfate reducing bacteria (SRB) through a dynamic tensile testing. Wu et al. evaluated the function of SRB on susceptibility to stress corrosion cracking (SCC) of X80 steel. The investigation demonstrated that SRB increased the SCC susceptibility of the steel, it also promoted the plasticity loss[9]. Wu et al. researched the influence of SRB on mechano-chemical effect of API 5L X80 steel. The results showed that the SRB physiological activity, strain rate and strain can influence the mechano-chemical effect of the steel[10]. However, there are few studies evaluating the mechanical behavior of this steel after a long period of exposure to the microorganisms under static conditions. This research aimed to analyze the plastic deformation of API 5L X80 steel coupons after 360 days of exposure to the produced water systems (abiotic and biotic). Coupons were analyzed chemically and metallographically. The mechanical behavior of the steel was investigated through tensile tests and fractographic analysis. The three-dimensional

*e-mail: edkarllaquimica@hotmail.com

(3D) topography and roughness of the surfaces after the corrosion process were assessed by Confocal Laser Scanning Microscopy (CLSM).

2. Experimental Procedure

2.1 Material and microstructural characterization

The material used was obtained from a API 5L X80 pipeline steel, with the following chemical composition (wt%): 0.08 C, 0.3 Si, 1.82 Mn, 0.009 P, 0.001 S, 0.17 Cr, 0.01 Ni, 0.20 Mo, 0.01 Cu, 0.037 Al, 0.024 V, 0.003 W, 0.021 Ti, 0.081 Nb and balance Fe. Coupons were made in the dimensions of 30 x 10 x 5 mm for the tests. For the microstructural characterization, the coupons were sanded with sandpaper (220-1200 mesh) and polished with diamond paste (3 and 1 µm), cleaned in isopropyl alcohol and acetone, and dried with a hot air jet. Subsequently, the coupon surface was attacked with 2% nital reagent for 10 seconds in order to identify the microconstituents in a Scanning Electron Microscope (SEM) HITACHI TM 3000. A microstructure consisting of acicular ferrite (AF) and polygonal ferrite (PF) is shown in Figure 1. Coupons for the tensile test were sectioned longitudinally parallel to the direction of lamination of the tube having the dimensions as shown in Figure 2.

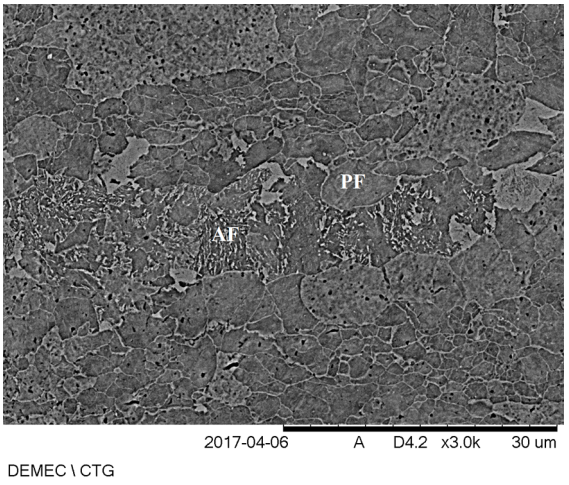

Figure 1. Microstructure of API 5L X80 steel showing acicular ferrite (AF) and polygonal ferrite (PF).

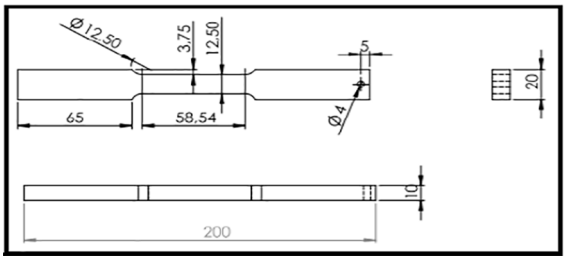

Figure 2. Schematic diagram of the coupon used in the tensile test.

2.2 Testing medium

Produced water was obtained from an oilfield located in Northeast Brazil. The experiments were conducted on two open static test cells (abiotic and biotic systems) with produced water for 360 days at room temperature (~25 °C), according to Figure 3. In the abiotic system, the disinfection condition was established after the microfiltration of the produced water through membranes with 0.2 µm pores, followed by the addition of 1 mg/L of sodium hypochlorite. For the biotic system, produced water as it was received was used, with no treatment presenting normal microbiota.

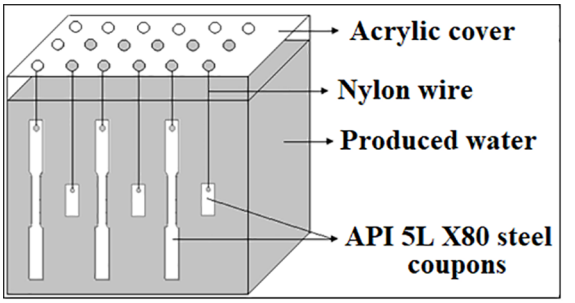

Figure 3. Schematic diagram of the static systems used in the experiments.

2.3 Methods of quantification and culture of microorganisms

The groups of total anaerobic, acid-producing aerobic and anaerobic bacteria and sulfate reducing bacteria (SRB) were quantified using the Most Probable Number (MPN) method[11]. While, total aerobic and precipitating iron bacteria were quantified by the Colony Forming Unit (CFU) method[12,13]. Planktonic microorganisms were quantified from the inoculum of 1 mL of produced water in reducing solution, followed by re-inoculation in the respective culture media. The sessile microorganisms were quantified by removing the biofilm from the surface of the coupons with a non-metallic spatula in reducing solution, followed by 1 mL inoculum of this solution in the respective culture media.

The composition of the culture medium of the microorganisms are given in Table 1. Culture medium from anaerobic microorganism groups were purged with nitrogen before sterilization in autoclave. The reducing solution contained the following constituents in (g/L): 30.0 NaCl, 0.124 sodium thioglycolate, 0.1 ascorbic acid and 4.0 mL resazurin (0.025%) (pH 7.6). All components were per liter of distilled water. All groups of microorganisms were incubated at 35 ºC. All culture media and solutions were sterilized in autoclave at 121 ºC for 20 minutes.

Table 1. Composition of the culture medium of different groups of microorganisms.

Group of microorganisms	Composition in (g/L) of the culture medium	pH
Total aerobic	30.0 NaCl and 22.5 Plate Count Agar (PCA) medium	7.0
Total anaerobic	30.0 NaCl and 30.0 fluid medium thioglycolate	7.0
Acid-producing aerobic and anaerobic	30.0 NaCl, 10.0 sucrose, 10.0 tryptone, 1.0 beef extract and 0.018 phenol red	7.2
Iron-precipitating bacteria	30.0 NaCl, 0.5 $(NH_4)_2SO_4$, 0.2 $CaCl_2.2H_2O$, 0.5 $MgSO_4.7H_2O$, 0.5 $NaNO_3$, 10.0 ferric ammonium citrate and 0.5 K_2HPO_4	7.0
SRB	30.0 NaCl, 0.5 KH_2PO_4, 1.0 NH_4Cl, 1.0 Na_2SO_4, 0.67 $CaCl_2.2H_2O$, 1.68 $MgCl_2.6H_2O$, 7.0 mL sodium lactate (50%), 1.0 yeast extract, 0.1 ascorbic acid, 1.9 agar-agar, 4.0 mL resazurin (0.025%) and 0.5 $FeSO_4.7H_2O$	7.6

2.4 Surface analysis by laser confocal microscopy

The surface of the API 5L X80 steel coupons was evaluated before exposure and after 360 days of immersion in the abiotic system (formation and removal of the film) and in the biotic system (formation and removal of the biofilm) using the laser confocal microscope Zeiss Axio Imager Z2m. To remove any preexisting corrosion and standardize roughness, before exposure, all coupons were blasted with glass microspheres, washed with isopropyl alcohol and acetone, and dried with air jets. Three-dimensional and roughness analyzes were performed at the center (X: 15.000 µm and Y: 5.000 µm) of the coupon (dimensions of 30 x 10 x 5 mm) with an area of 640.000 μm^2. Seven profiles were measured so as to obtain the mean roughness (Ra), mean roughness deviation (Rq), and skewness and kurtosis parameters. To examine the extent of corrosion, the films and biofilms formed on the surface of the coupons were removed by a non-metallic spatula. After this procedure, the coupons were immersed in Clark solution, followed by ultrasonic cleaning in distilled water. Thereafter, they were cleaned in isopropyl alcohol and acetone, and dried with air jets, according to ASTM G1-03 standard[14]. As the present work is part of a series of studies, the methodology of weight loss and corrosion rate has already been published[15].

2.5 Tensile test and fractographic analysis

The tensile tests were performed on the coupons without exposure (control) and after 360 days of exposure to the abiotic and biotic systems, in triplicate. The strain was measured over a length of 50 mm using an extensometer (EMIC model EE09). The tests were performed on EMIC DL 10000 using a 10.000 kgf load cell with test speed of 2 mm/min. The tensile tests were evaluated according to ASTM E8/E8M – 15a standard[16]. After the tests, the fracture of the surface was analyzed in the SEM HITACHI TM 3000.

3. Results and Discussion

3.1 Microbiological quantification

Table 2 shows the microbiological quantification of the different groups of microorganisms present in the produced water and the biofilm formed on the surface of the coupon after 360 days.

Among the groups investigated (Table 2), only the precipitating iron bacteria were not present in the produced water initially, however, after 360 days this group was detected in the biofilm formed on the carbon steel. This result may be related to the low cellular concentration of these bacteria in produced water for their growth was not observed after the time determined by the plate count method. Over time, as the oxidation of steel occurred, it was solubilized in the produced water, making it available to be metabolized by previously dormant bacteria. This resulted in the detection of precipitating iron bacteria after 360 days. However, this group of bacteria was identified in sessile microbiological quantification studies after 15 days (not shown here). The biomineralization of iron by precipitating iron bacteria occurs through oxidation reactions by converting the ferrous ion (Fe^{2+}) to ferric (Fe^{3+}) and oxygen as a final electron acceptor[17]. After 360 days, only acid-producing aerobic bacteria were not detected in produced water possibly due

Table 2. Quantification of the planktonic microorganisms present in the produced water and sessile adhered to the film after 360 days.

Group of microorganisms	Count of planktonic microorganisms	Count of sessile microorganisms
Total aerobic	1.2 x 10^4 CFU/mL	6.6 CFU/cm^2
Total anaerobic	1.1 x 10^3 MPN/mL	1.4 x 10^3 MPN/cm^2
Acid-producing aerobic	7.0 x 10 MPN/mL	Undetected
Acid-producing anaerobic	2.5 x 10^2 MPN/mL	4.1 x 10^1 MPN/cm^2
Iron-precipitating bacteria	Undetected	2.6 x 10^1 CFU/cm^2
SRB	4.5 x 10^3 MPN/mL	1.4 x 10^3 MPN/cm^2

to nutrient depletion or the development of inhospitable conditions over time.

3.2 3D topography and surface roughness analysis of coupons

Figure 4 shows the three-dimensional topographies of the surfaces of the API 5L X80 steel coupons by confocal laser microscopy under the following conditions: before exposure and after 360 days of exposure to abiotic systems (with and without films) and biotic (with and without biofilms).

When correlating the steel images before exposure (Figure 4 (A) and (B)) with the respective images of the steels after 360 days of exposure (Figure 4 (A1) and (B1)), it can be observed that the topographies of films and biofilms were different. The coupon exposed to the abiotic system formed an irregular, less thick film composed of deposited salts and minimal amount of corrosion products (Figure 4 (A1)). Meanwhile, there was the formation of thicker biofilms and corrosion products with a non-uniform distribution overlying the metal surface exposed to the biotic system (Figure 4 (B1)). The surface shown in Figure 4 (A2) is practically unchanged

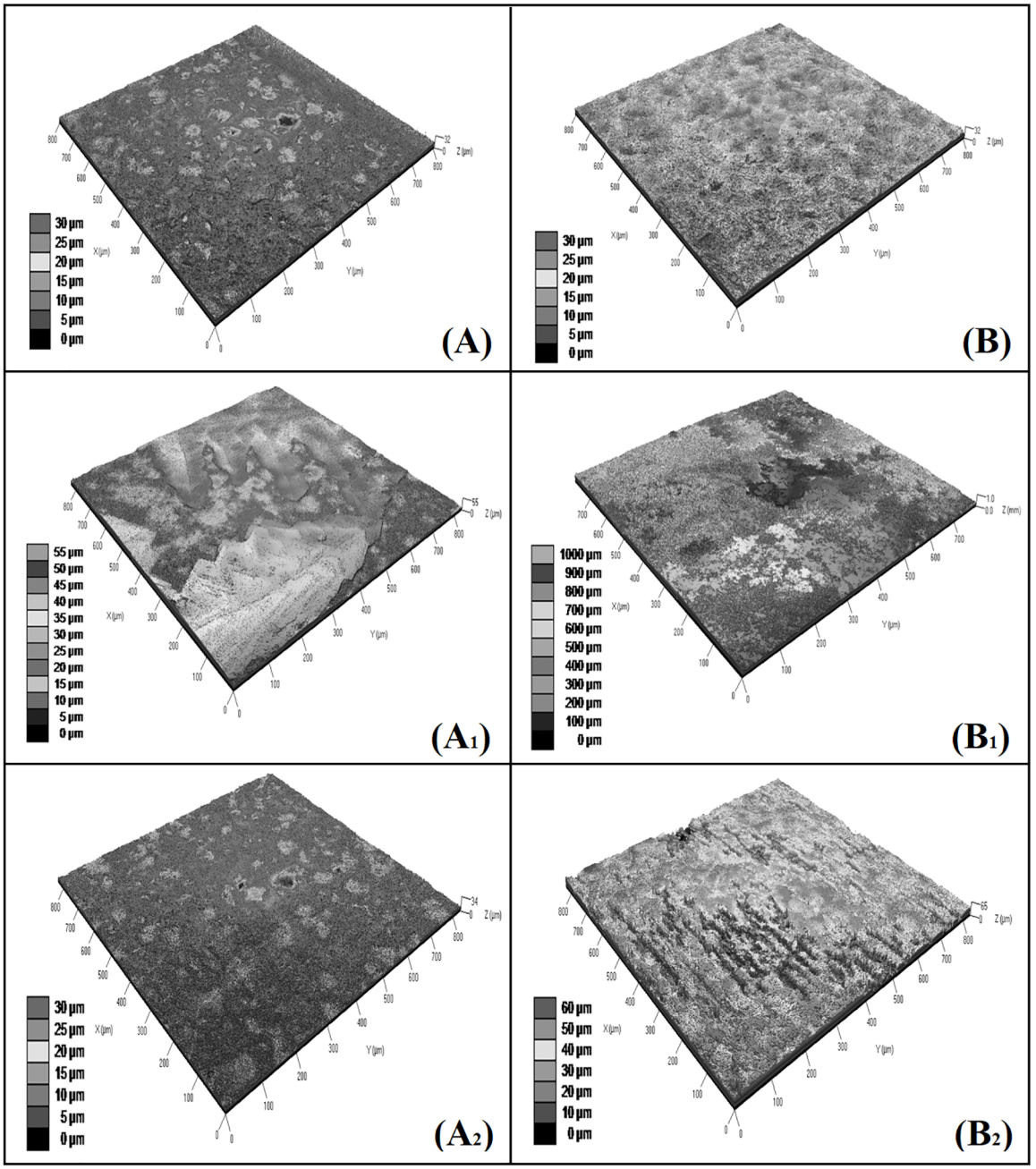

Figure 4. 3D topographies of API 5L X80 steel coupons. (A) abiotic before exposure, (A1) abiotic after exposure with film, (A2) abiotic after exposure without film, (B) biotic before exposure, (B1) biotic after exposure with biofilm and (B2) biotic after exposure without biofilm.

when compared to the image of the steel exposed to the abiotic system (Figure 4 (A)). This result corroborates the low weight loss values (0.018%) and corrosion rate (0.029 mm/year) for the abiotic system after 360 days of exposure. Comparing the surface after the removal of the biofilm and corrosion products (Figure 4 (B2)) with the image of the steel exposed to the biotic system (Figure 4 (B)) it can be seen that some surface regions remained flat and other excavations and deep grooves were directed towards the lamination. During the rolling process, the grain is stretched in the direction of rolling, which may cause residual stresses to accumulate with preferred corrosion action[18]. In addition, coupons from the biotic system showed higher weight loss (2.66%) and corrosion rate (0.0407 mm/year) than coupons from the abiotic system. The metabolic activity of the microorganisms in the produced water (biotic system) favored the corrosion process of X80 steel. It was not possible to identify the corrosion pits in Figure 4 (B2), because of the long exposure time of the steel to the biotic system, which caused the formation of craters and deep grooves in the surface in the final time studied. Research shows that throughout short periods of immersion deep pits with smaller surface area can be formed. When the immersion time is increased, the formed pits became extremely shallow with a larger surface area. These shallow pits alter the mechanochemical activity of the steel through the accumulation of tension at the edge of the pits causing preferential dissolution in the direction parallel to the steel surface. This fact increases the growth rate of pits and coalescence of neighboring pits[19,20]. The mean roughness (Ra), mean square deviation (Rq) values, the statistical parameters of skewness (Rsk) and kurtosis (Rku) shown in Table 3 were obtained through topographic images.

In Table 3 it can observed that the values of Ra and Rq were very close to both surfaces in the prior to exposure condition, as a result of the blasting of the coupons. After 360 days, the Ra and Rq of the film and biofilm coupons were larger in relation to the respective coupons before exposure due to the greater variation between the height of the peaks and the depth of the valleys formed in the final configuration of the film and biofilm. After removing the film from the surface exposed to the abiotic system, it was observed that the value of Ra presented a small variation in comparison to the control condition, corroborating the low corrosion observed in this system through the values of weight loss and corrosion rate. The high deviation observed in the Ra value of the surface exposed to the biotic system with biofilm is associated with non-uniformity of deposition during the dynamic process of formation of this biofilm. The values of Ra and Rq of the surface without biofilm exposed to the biotic system were higher in relation to the without film surface of the abiotic system. This increase in the roughness values is due to the more severe corrosion caused by the consortium of microorganisms associated to the differential aeration that occurred after the formation of the biofilm on the surface of the coupons exposed to the biotic system. In most investigations on surface roughness characterization only the Ra and/or Rq parameters are investigated. The analysis of the roughness conducted only by these two measures presents limitations, being necessary to use one or more spatial parameters of height like Rsk and Rku[21-23]. On the non-exposed surfaces, the Rsk was greater than zero (positive skewness) indicating that the blasting had high peaks with broad and shallow valleys. After the period of exposure to the produced water (with and without film or biofilm), the Rsk was less than zero (negative skewness), showing that the surfaces after the corrosion process presented small peaks with deep and narrow valleys[23]. The surfaces of the control coupons and whithout film presented Rku less than three, denoting a surface with few high peaks and low valleys which are characteristic of a platicuric distribution (curve flatter than the normal distribution). On the surfaces of the biofilm coupons of the biotic system, and after the removal of the films and biofilms, Rku was observed to be higher than three, indicating that the distribution of the curve was leptokurtic (curve sharper than the normal distribution), with many high peaks and valleys[21].

3.3 Result of the tensile test

The graph of stress (σ) versus strain (ε) of API 5L X80 steel coupons without exposure (control) and after 360 days of exposure to the abiotic and biotic systems is presented in Figure 5. The mean values of the results obtained in the tensile test along with the standard deviation are given in Table 4.

In Figure 5, stress-strain curves of API 5L X80 steel coupons exhibit similarity in the elastic deformation region. The curves showed no discontinuities between the elastic and plastic regions. So as to analyze the data in Table 4, it

Table 3. Analysis of surface roughness of API 5L X80 steel coupons.

Sistems	Ra (µm)	Rq (µm)	Rsk	Rku
Abiotic (before exposure)	2.15 ± 0.25	2.59 ± 0.32	0.31 ± 0.10	2.53 ± 0.48
Biotic (before exposure)	2.24 ± 0.26	2.81 ± 0.28	0.34 ± 0.15	2.98 ± 0.57
Abiotic (with film)	7.88 ± 1.45	9.06 ± 0.24	-0.08 ± 0.01	1.84 ± 0.24
Biotic (with biofilm)	120.86 ± 18.43	148.32 ± 0.42	-0.46 ± 0.03	3.19 ± 1.14
Abiotic (without film)	1.43 ± 0.20	1.81 ± 0.26	-0.43 ± 0.12	3.37 ± 0.47
Biotic (without biofilm)	7.43 ± 0.99	9.37 ± 0.95	-1.23 ± 0.30	3.85 ± 0.86

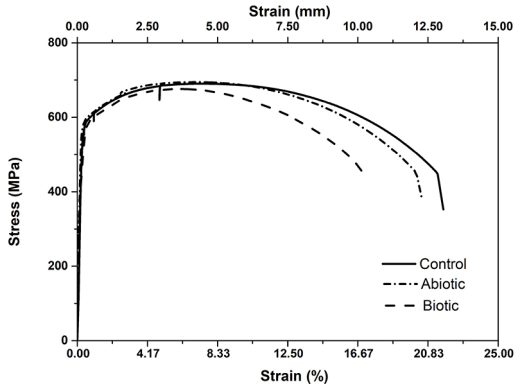

Figure 5. Stress-strain curve of API 5L X80 steel coupons in periods without exposure (control) and after 360 days of exposure to abiotic and biotic systems.

was necessary to consider the weight loss which occurred in the coupons from the corrosion process. Before exposure to the systems, the coupons had a cross section of 12.5 x 10 mm (125 mm^2 area) as shown in Figure 2. After exposure to the systems, there was a variation in the coupon cross sectional area owing to weight loss. Considering this variation, the maximum tensile strength and yield strength parameters were corrected. The maximum tensile strength was extracted using the following equation: $\sigma_{corrected} = \frac{F}{S_F}$, where $\sigma_{corrected}$ is corrected stress, F is the force measured during tensile test and S_F is the final corrected cross sectional area. Due to non-uniform corrosion (pits), the real cross sectional area can´t be obtained by measuring the coupons external dimensions. In this paper, the cross section was corrected with a view to estimating the real cross section. Therefore, the percentual weight loss was subtracted from the initial cross section area. The same correction was applied on the yield strength. The yield strength was calculated using the following equation: $\sigma_e = \frac{F_e}{S_0}$, where σ_e is stress at 0.2% elongation and F_e is yield strength, that is, the force measured for a 0.2% elastic elongation. The steels exposed to the abiotic and biotic systems presented weight loss values of 0.18% (124.77 mm^2 area) and 2.66% (121.67 mm^2 area), respectively. After correction, the maximum tensile strength values for the abiotic and biotic systems were 695.8 ± 1.5 MPa and 694.4 ± 0.6 MPa, respectively, and yield strength values were 567.1 ± 11.3 MPa and 574.7 ± 3.4 MPa, respectively. As shown, no variation was observed between maximum tensile strength and yield strength coupons exposed to the abiotic and biotic systems compared to the control (no exposure) shown in Table 4. Through this data, it can be concluded that the microorganism in the produced water have no influence on the mechanical properties of API 5L X80 steel. However, the literature shows that SRB have different mechanisms (anodic dissolution augmented by the concentration of metabolically generated sulphide; sulfate reduction leads to increased cathodic current density in cathode depolarization; pitting corrosion caused by the direct transfer of electrons and by reduced sulfur compounds) which alter the mechanical properties of X80 steel[9]. This difference between behaviors may be explained by the correction made on the cross section area in this paper. Without correction on the coupons cross section and using the initial cross sectional area in stress calculations, the stresses will be lower for coupons exposed to corrosion. The cause of this behavior in the material is not the loss in mechanical properties, but the reduction of the requested cross sectional area. This reduction is caused by corrosion. With a smaller cross section area, the force F supported by the coupon is smaller. Since the stress calculation is F/S and the initial area is larger than in reality, the stress is smaller. However, the stress is actually the same when the section area after corrosion is considered. Considering the plastic region of the curves shown in Figure 5 it can be seen that they exhibited similar behaviors. Lower values of total elongation (Table 4) were observed for the coupon exposed to the biotic system (9.8% ± 0.4), when compared to the control coupon (21.0% ± 0.3) and exposed to the abiotic system (19.8% ± 0.2). The coupon exposed to the biotic system presented a reduction in plasticity when compared to the other two conditions. This behavior can be attributed to the formation of corrosion pits on the surface of the coupons induced by the microorganisms present in the produced water. Images showing pitting corrosion on API 5L X80 steel coupons with up to 60 days of exposure to the biotic system have been published[15]. The high density of pits induced by the physiological activity of SRB is a very important factor in the alteration of the plasticity of the X80 steel coupons. As a consequence of the formation of pits, the tension accumulates at the bottom of the corrosion pit during the tensile test. Subsequently, there is the emergence of micro-cracks that propagate in the direction perpendicular to the charge, and extend to the surface of the metal[10]. Because of the pits and the tension concentrations at the bottom of the pits, the emergence and propagation of micro-cracks to free surfaces occur earlier, for there is less deformation.

Table 4. Mean of the results obtained in the tensile tests.

Sistems	Maximum tensile strength (MPa)	Yield strength (MPa)	Strain maximum tensile (%)	Total elongation (%)
Without exposure (control)	697.8 ± 1.7	589.2 ± 9.1	7.1 ± 1.4	21.0 ± 0.3
Abiotic	694.6 ± 1.5	566.1 ± 11.3	6.9 ± 1.0	19.8 ± 0.2
Biotic	676.0 ± 0.6	559.9 ± 3.4	6.6 ± 0.9	9.8 ± 0.4

3.4 Result of the fractographic analysis

The fractographic analyzes of the API 5L X80 steel coupons in the periods without exposure (control) and after 360 days of exposure to the abiotic and biotic systems are presented in Figure 6. The areas analyzed in the fractografic images were marked with white rectangles.

Microscopically, the rupture observed in the samples was ductile in all coupons, exhibiting microvoids and microcavities that coalesced into the dimples, which is characteristic of plastic shear deformations (Figure 6). At the beginning of the deformation, there was a growth of these microvoids and small cavities, which with the continuity of the deformation, united and coalesced

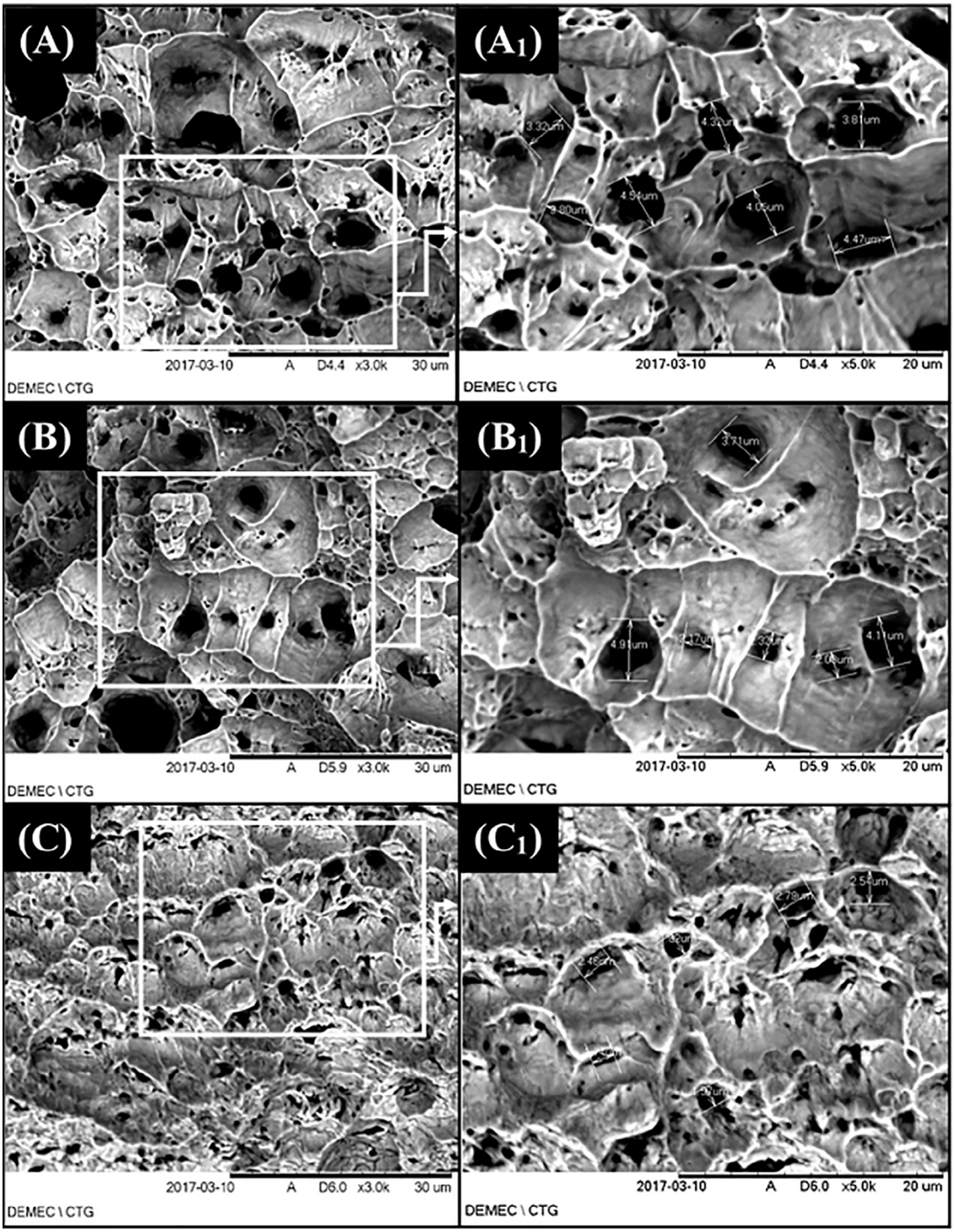

Figure 6. Fractography of API 5L X80 steel coupons. Under the conditions: (A and A1) control, (B and B1) abiotic and (C and C1) biotic.

forming micro-cracks, which later caused the rupture of the central region of the steel[10]. The fractography of the biotic system presented in Figure 6 (C and C1) showed dimples with smaller diameters (2.15 μm ± 0.52), when compared to the control system dimples (4.04 μm ± 0.40) (Figure 6A and A1) and in the abiotic system (3.21 μm ± 1.25) (Figure 6B and B1). A tendency to reduce the diameter of the dimples can be observed when the coupon was exposed to the biotic system. The metabolites produced by the microorganisms and the formation of cells of differential aeration in the biotic system caused the formation of pits. Pits are micro defects on the surface of coupons that accumulate tension and promote crack propagation resulting in decreased coupon plasticity. With the reduction of plasticity, the elongation of the coupon until rupture is smaller. Hence, the diameter of the observed dimples is smaller. These results can be explained by the plasticity loss observed during the tensile test. Dimples size are proportional to coupons deformation. With smaller deformation before rupture, smaller dimples are generated on coupons exposed to the biotic system, as it can be observed Figure 6C and C1.

4. Conclusions

In this study the plastic deformation of API 5L X80 steel coupons submitted to the microbiological activity of the produced water was investigated. The topographic 3D analysis of the corroded surface of the biotic system revealed greater damage (excavations and deep grooves) caused by the aggressive metabolites produced by the microorganisms during the formation of the biofilm associated to the corrosion process, in relation to the other two systems. The roughness values Ra and Rq were higher for the coupon exposed to the biotic condition denoting a higher corrosive action of this system. The results of the tensile test showed similarity in the behavior of the steel in all test conditions after analyzing the cross sectional area variation. There is a need to evaluate the cross sectional area of coupons before and after the tensile test considering weight loss. Studies of the fracture surface of the coupons exposed to the biotic system revealed a reduction in the diameter of the dimples characterizing loss of plasticity. The microorganisms present in produced water tend to generate corrosion pits which decrease coupons plasticity and, consequently, dimples size. Meanwhile, the coupons exposed to the abiotic system presented dimples size very close to the control condition.

5. Acknowledgements

The authors would like to acknowledge the support received from the Programa de Recursos Humanos da Petrobras (PRH-203), CAPES, CNPq and Finep.

6. References

1. American Petroleum Institute (API). *ANSI/API Specification 5L/ISO 3183 – Petrolum and natural gas industries – Steel pipe for pipeline transportation systems*. Washington, DC: API; 2007.

2. Aydin H. Relationship between a bainitic structure and the hardness in the weld zone of the friction-stir welded X80 API-grade pipe-line steel. *Materials and Technology*. 2014;48(1):15-22.

3. Al-Abbas FM, Spear JR, Kakpovbia A, Balhareth NM, Olson DL, Mishra B. Bacterial attachment to metal substrate and its effects on microbiologically-influenced corrosion in transporting hydrocarbon pipelines. *Journal of Pipeline Engineering*. 2012;11(1):63-72.

4. Javaherdashti R, Ramanb RKS, Panterc C, Pereloma EV. Microbiologically assisted stress corrosion cracking of carbon steel in mixed and pure cultures of sulfate reducing bacteria. *International Biodeterioration and Biodegradation*. 2006;58(1):27-35.

5. Clarck CE, Veil JA. *Produced water volumes and management practices in the United States – Environmental Science Division. Report ANL/EVS/R-09/1*. Lemont, IL: Argonne National Laboratory; 2009.

6. Albuquerque AC, Andrade C, Neves B. Biocorrosão: da integridade do biofilme à integridade do material. *Corrosão e Protecção dos Materiais*. 2014;33(1-2):18-23.

7. Wu T, Xu J, Yan M, Sun C, Yu C, Ke W. Synergistic effect of sulfate-reducing bacteria and elastic stress on corrosion of X80 steel in soil solution. *Corrosion Science*. 2014;83:38-47.

8. Wu T, Xu J, Sun C, Yan M, Yu C, Ke W. Microbial corrosion of pipeline steel under yield stress in soil environment. *Corrosion Science*. 2014;88:291-305.

9. Wu T, Yan M, Zeng D, Xu J, Sun C, Yu C, Ke W. Stress corrosion cracking of X80 steel in the presence of sulfate-reducing bacteria. *Journal of Materials Science and Tecnology*. 2015;31(4):413-422.

10. Wu T, Yan M, Xu J, Liu Y, Sun C, Ke W. Mechano-chemical effect of pipeline steel in microbiological corrosion. *Corrosion Science*. 2016;108:160-168.

11. Postgate JR. *The sulphate-reducing bacteria*. 2nd ed. Cambridge: Cambridge University Press; 1984.

12. Tortora GJ, Funke BR, Case CL. *Microbiologia*. Porto Alegre: ArtMed Editora; 2000.

13. Companhia Ambiental do Estado de São Paulo (CETESB). *Norma L5.201 – Contagem de bactérias heterotróficas: método de ensaio.* São Paulo: CETESB; 2006.

14. American Society for Testing and Materials (ASTM). *ASTM G1-03 – Standard practice for preparing, cleaning, and evaluating corrosion test specimens*. West Conshohocken, PA: ASTM International; 2011.

15. Oliveira ESD, Pereira RFC, Melo IR, Lima MAGA, Urtiga Filho SL. Corrosion behavior of API 5L X80 steel in the produced water of onshore oil recovery facilities. *Materials Research*. 2017;20(Suppl 2):432-9.

16. American Society for Testing and Materials (ASTM). *ASTM E8/E8M-15a – Standard test mehotd for tension testing of metallic materials.* West Conshohocken, PA: ASTM International; 2015.

17. Liu H, Gu T, Zhang G, Wang W, Dong S, Cheng Y, et al. Corrosion inhibition of carbon steel in CO2-containing oilfield produced water in the presence of iron-oxidizing bacteria and inhibitors. *Corrosion Science*. 2016;105:149-60.

18. Bresciani Filho E. *Conformação plástica dos metais*. São Paulo: EPUSP; 2011.

19. Alvarez RB, Martin HJ, Horstemeyer MF, Chandler MQ, Williams N, Wang PT, et al. Corrosion relationships as a function of time and surface roughness on a structural AE44 magnesium alloy. *Corrosion Science*. 2010;52(5):1635-48.

20. Yang Y, Zhang T, Shao Y, Meng G, Wang F. New understanding of the effect of hydrostatic pressure on the corrosion of Ni–Cr–Mo–V high strength steel. *Corrosion Science*. 2013;73:250-61.

21. Gadelmawla ES, Koura MM, Maksoud TMA, Elewa IM, Soliman HH. Roughness parameters. *Journal of Materials Processing Technology*. 2002;123(1):133-145.

22. Ivanova EP, Truong VK, Wang JY, Berndt CC, Jones RT, Yusuf II, et al. Impact of nanoscale roughness of titanium thin film surfaces on bacterial retention. *Langmuir*. 2010;26(3):1973-82.

23. Crawford RJ, Webb HK, Truong VK, Hasan J, Ivanova EP. Surface topographical factors influencing bacterial attachment. *Advances in Colloid and Interface Science.* 2012;179-182:142-9.